

# Spatial Reasoning with Incomplete Information on Relative Positioning

Sidi Mohammed Réda Dehak, *Member, IEEE*, Isabelle Bloch, *Member, IEEE*, and Henri Maître, *Member, IEEE*

**Abstract**—This paper describes a probabilistic method of inferring the position of a point with respect to a reference point knowing their relative spatial position to a third point. We address this problem in the case of incomplete information where only the angular spatial relationships are known. The use of probabilistic representations allows us to model prior knowledge. We derive exact formulae expressing the conditional probability of the position given the two known angles, in typical cases: uniform or Gaussian random prior distributions within rectangular or circular regions. This result is illustrated with respect to two different simulations: The first is devoted to the localization of a mobile phone using only angular relationships, the second, to georeferencing within a city. This last example uses angular relationships and some additional knowledge about the position.

**Index Terms**—Probabilistic geometry, spatial reasoning, geometrical inference.

## 1 INTRODUCTION

HUMAN beings have the amazing capability of being able to find their way using very incomplete references. For instance, when visiting a city, one may find without (too much) difficulty the small souvenir shop “in the direction of the cathedral” and “on the left when walking toward the sea.” Such an ability may be called “spatial reasoning.” Indeed, spatial reasoning consists in representing knowledge concerning spatial entities and spatial relationships and reasoning on them. It is different from classical geometrical reasoning which, for instance, allows the third side of a triangle, of which two sides and an angle are known, to be calculated. To address the common tourist problem presented above, our reasoning is made up of several deductions derived under uncertainty and incomplete information.

In the first instance, the pieces of information are not accurate. “On the left of” and “in the direction of” are instances of information which have no exact value. They convey a rather loose meaning which may be interpreted in different ways depending on the context [1]. These elements carry the “uncertainty” aspect of the spatial information dealt with in spatial reasoning.

Furthermore, no piece of information is complete enough to solve the reasoning problem at hand entirely. Each one provides a degenerated solution (to a localization problem, for instance), where a large part of space is acceptable. This constitutes the “incomplete” aspect of spatial information. We expect that combining these pieces of information will somewhat reduce the level of uncertainty. But, how can we combine such elements which do not share any common

reference and can hardly be projected in a consistent framework? This is the objective of this paper which primarily addresses the “incompleteness” of spatial information, more than its “uncertainty.”

In Section 2, we present previous work devoted to reasoning with spatial information. We first present a brief overview of the literature dealing with uncertainty reduction and information compounding. We subsequently deal with spatial knowledge representation with emphasis on the two aspects of quantitative and qualitative representations. The problem we are trying to solve is precisely stated and formalized in Section 3. In particular, we detail the cases where we have reduced prior information and we assume that points are uniformly distributed in a bounded space (circle or rectangle) in Section 4, or follow a Gaussian distribution in Section 5 according to some prior information. Inference is then performed in a Bayesian framework (Section 6). Two illustrative examples are described in Section 7, one dealing with small objects such as in the case of localization of mobile phones, and one addressing the problem of georeferencing in a city.

## 2 RELATED WORK

### 2.1 Spatial Reasoning under Uncertainty and Compounding for Position Estimation

Although uncertainty management is not the primary goal of this paper, it is worth mentioning the attempts at dealing with uncertainty on positioning and combining uncertain measurements on relative position. Indeed, a large body of literature addresses this problem, in particular, in the robotics community. Mobile robotics is a typical domain where uncertainty degrades the robot’s knowledge about the geometry of its environment [2], [3], [4].

Since the early work based on error modeled as Gaussian distributions or covariance matrices (see, e.g., [5], [6]), and on the notion of occupancy grid [7] and position probability grid [8], several solutions have been proposed in order to take into account successive relative position estimates. In

• S.M.R. Dehak is with EPITA-LRDE, 14-16 rue Voltaire, 94276 Le Kremlin-Bicetre Cedex, France. E-mail: reda@lrde.epita.fr.

• I. Bloch and H. Maître are with GET-Telecom Paris-CNRS UMR 5141 LTCI, 46 rue Barrault, 75013 Paris, France. E-mail: {Isabelle.Bloch, Henri.Maître}@enst.fr.

Manuscript received 23 Dec. 2003; revised 23 Aug. 2004; accepted 20 Dec. 2004; published online 14 July 2005.

Recommended for acceptance by D. Fleet.

For information on obtaining reprints of this article, please send e-mail to: tpami@computer.org, and reference IEEECS Log Number TPAMI-0445-1203.

[4], stochastic maps are built under complete but uncertain spatial information. A stochastic map consists of two features: The first represents spatial relationships (distance and angle) reflecting the spatial location of object with respect to the world reference frame, and the second is an associated covariance matrix which models the uncertainty of each location. Using an algebraic composition of approximate estimates, the authors propose a procedure to build this map, extract information from it, and update it incrementally as new information (a new object or a new constraint) is obtained. Successive sensor measurements lead to uncertainty reduction. In this work, the distance information plays an important role. Other approaches assume a known environment, or a model of it. Positioning is then achieved by matching estimates from measurements and the model. Active sensing allows a position probability grid to be updated, for instance, using Markovian error estimation [9]. Other methods use Kalman filters to track observed beacons and match them with a prior map of their location [10], or geometric reasoning with complex numbers in order to solve the triangulation problem with respect to noisy data and matching with the environment map [11].

Note that in several of these robotics problems, incompleteness of information is not the central issue. Incomplete measures are often obtained, for instance, when localizing is performed only with respect to the directions of landmarks. But, under these constraints, several landmarks are usually combined to provide an estimate of the sensor position.

An interesting issue is addressed in [12]: The authors propose a linear programming technique able to efficiently solve one part of the problem we propose, namely, the determination of the admissible domain of localization. The position is bounded by some angular sector and range limits, which define constraints on the possible set of positions. Several such constraints in multirobot applications are combined and lead to a polytope. We will make use of some of these results. In case of incomplete information, for instance, when only angular information is available, we can extend this work by considering the uncertainty domain as an angular sector, infinite in range.

A dual problem was addressed in [13] for mobile communication optimization where the range of information is bounded, but no information is available on angular positions. This is obtained by exploiting the connectivity of the network which imposes constraints on node proximity. The problem is expressed in terms of linear matrix inequalities and solved by convex optimization. Furthermore, because it only focuses on the solution domain, the method reaches its limits in case of loose constraints (i.e., important incompleteness). In this case, it provides one possible solution, but does not guarantee that the most likely ones are exhibited. As mentioned by the authors, angular information has to be introduced to achieve a better degree of convergence.

## 2.2 Further Approaches in Spatial Knowledge Representation and Spatial Reasoning

Several other scientific communities have addressed the problem of spatial knowledge representation. Two main classes of methods can be distinguished. The first consists of qualitative representations and are usually based on formal logics [14], [15]. Typically, spatial entities are elements of language or propositional terms, while relationships are expressed as operators, modalities, etc. (see, e.g., [14] for a

survey). The second class consists of (semi)quantitative approaches and are often based on fuzzy set or probability theories. While qualitative methods are most often applied to geographic information systems (GIS) and natural language processing, quantitative approaches are mostly found in image processing, computer vision, and robotics.

As far as directional relations are concerned, qualitative representations are less developed than for topological relationships. Cardinal directions (i.e., North, South, East, and West) are used in [16]. Other approaches are inspired by the temporal interval representations [17], and one of the most used representations (in particular in GIS) is 2D strings [18] which use relations between the projections of the considered objects on two orthogonal axes and interval-based representations on each axis. Finally, we mention the approach in [19] which represents the relative position of a point with respect to two other points as a  $5 \times 3$  matrix based on a subdivision of the space into six sectors related to the two reference points.

Quantitative representations of directional relations are more developed and try to define how expressions such as "to the left of" can be quantified. The ambiguity of such relations lead to fuzzy representations, already suggested in [20]. Most existing methods for defining fuzzy relative spatial positions rely on angular measurements between points of the two objects of interest [21], [22] and concern 2D objects. A fuzzy relationship is defined as a fuzzy set, and the correspondence between the relationship and the angle measurements is then evaluated. A method based on linear cross-sections of the objects instead of just points has been developed in [23]. Finally, methods based on whole objects have been proposed, based either on learning from human evaluation [24], on projections of the objects [25], or on a morphological approach [26]. A detailed comparison of these approaches can be found in [27]. Besides these knowledge representation approaches, probabilistic models have been largely developed, as described in Section 2.1.

While the problem of inference and reasoning about spatial relations [28] has been widely addressed in logical and qualitative representations, where the strong apparatus of formal logic is very useful, there has been less development when quantitative representations are used. Some geometric reasoning approaches in a probabilistic framework or on linear constraints have been developed, as described above, as well as methods based on fuzzy logic (see, e.g., [29]). Detailing these methods is beyond the scope of this paper.

A large source of inspiration for knowledge representation and reasoning is found in the literature on linguistics and cognitive science (see, e.g., [1]). Interestingly enough, spatial language is rather nonmetric (or metric information is digitized in a very rough way), but intensively uses directions, mainly, three coordinate axes [30]. This advocates reasoning processes based on linguistic descriptions of a scene or a situation where distance plays almost no role. A remarkable feature of linguistic expressions is that representation and communication are then achieved without using numbers.

## 2.3 Outline of the Proposed Approach

In this paper, we use a quantitative representation of spatial uncertain information based on probabilities and propose a contribution to spatial reasoning and inference under

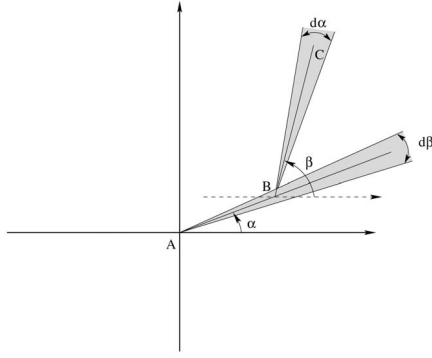


Fig. 1. Problem 1 may be stated as: “Where is point  $C$  with respect to  $A$ , knowing that it is in direction  $\beta$  with respect to an unknown point  $B$ , itself in direction  $\alpha$  with respect to  $A$ ?”

incomplete information. More specifically, we model the inference of the relations between two points from knowledge about the relations (angular position) of each of these points to a third point.

As in [12], we first compute the admissible domain. The main difference with respect to this work is that, instead of only considering the acceptability domain as a binary set, we compute a probability distribution on this domain. When no prior information is available on the objects, we use uniform or Gaussian prior distributions, which allow us to derive analytical expressions of the distributions. If prior information is available, it is modeled as specific distributions, which do not always lead to analytical solutions, but to numerical ones, as shown in our second example.

In summary, the main contribution of this paper is to show how complex spatial reasoning activities can be performed based on incomplete information (only angular information, no model or map) in a probabilistic framework and derive formal expressions in case of simple prior distributions. We illustrate the method on two examples, one with prior uniform distribution and the second showing how more complex information can be incorporated.

### 3 PROBLEM STATEMENT AND PROBABILISTIC FORMULATION

We consider the problem of localization where points are only known through the direction where they are with respect to a reference point and not through their distance to this point. More precisely, we address the simplest problem which may be stated as:<sup>1</sup>

**Problem 1.** *Let  $C$  be an unknown point. Let  $C$  be in the direction  $\beta$  from a point  $B$ , this point  $B$  being itself in the direction  $\alpha$  with respect to a reference point  $A$ . What can we say about the position of point  $C$  with respect to  $A$ ?*

We will demonstrate that, under rather loose assumptions, by assuming the statistical distribution of the unknown points, we may derive the exact distribution function of point  $C$  and propose good estimates of its relative positioning with respect to  $A$ . Statistical distributions of the unknown points reflect the prior knowledge of

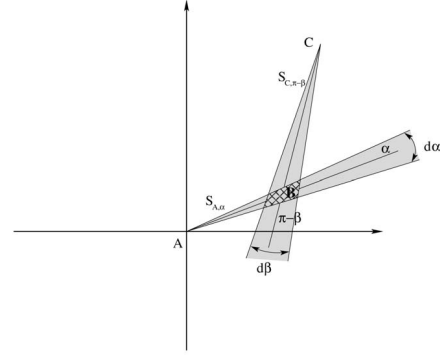


Fig. 2. Every point  $B$  in the dashed area fulfills the two conditions to be in direction  $\alpha$  with respect to point  $A$  (sector  $S_{A,\alpha}$ ) and to have point  $C$  in direction  $\beta$  (sector  $S_{C,\pi-\beta}$ ) within the respective tolerances  $\pm d\alpha/2, \pm d\beta/2$ .

the exact spatial position of these points. If no prior knowledge is available, the weakest assumption is made and we use a uniform distribution, which is the least committed distribution, derived from maximum entropy considerations [31], in the solution space.

We first introduce some notations. We choose, without loss of generality, point  $A$  as the origin of the Cartesian plane limited to some region (disk or square in the following). Any point  $M$  may be represented by its Cartesian coordinates  $x_M$  and  $y_M$ , or by its polar coordinates  $r_M$  and  $\theta_M$ . As a convention,  $r_M$  is a positive number and  $\theta_M$  belongs to  $[-\pi, \pi[$ . The notation  $[x \pm dx]$  denotes the interval  $[x - dx, x + dx]$ .

We consider that points  $M$  are distributed in the image according to a random distribution  $f_M(r, \theta)$ :

$$f_M(r, \theta) = \lim_{drd\theta \rightarrow 0} \frac{P(M : r_M \in [r \pm dr/2], \theta_M \in [\theta \pm d\theta/2])}{rdrd\theta}. \quad (1)$$

We will need in the sequel that  $f_M$  be an almost everywhere continuous function of the two variables  $r$  and  $\theta$ .

Fig. 1 represents the configuration expressed in Problem 1.

We are interested in the probability  $P(C, \alpha, \beta)$  which expresses the probability distribution of point  $C$  and the two angles  $\alpha$  and  $\beta$ . According to Fig. 2, this probability is equal to:

$$P(C, \alpha, \beta) = P(C) \int_{\Sigma} P(B) dB, \quad (2)$$

where  $\Sigma = S_{A,\alpha} \cap S_{C,\pi-\beta}$ , and  $S_{A,\alpha}$  and  $S_{C,\pi-\beta}$  are the two angular sectors described in Fig. 2.

The domain  $\Sigma$  is limited by four lines with equations:

$$r = r_c \frac{\sin[\theta_c - (\beta - \pi \pm d\beta/2)]}{\sin[\theta - (\beta - \pi \pm d\beta/2)]} \quad (3)$$

$$\theta = \alpha \pm d\alpha/2. \quad (4)$$

This domain is empty if  $\theta_c \notin [\alpha, \beta]$ . The probability  $P(C, \alpha, \beta)$  is equal to 0 for  $\theta_c \notin [\alpha, \beta]$ .

Denoting by  $g_{r,\theta}(\phi)$  the function of  $\mathbb{R} \rightarrow \mathbb{R}$ :

$$g_{r,\theta}(\phi) = r \frac{\sin[\theta_c - (\phi - \pi)]}{\sin[\theta - (\phi - \pi)]}. \quad (5)$$

1. Directions in the 2D space are defined by the angle with respect to the horizontal axis.

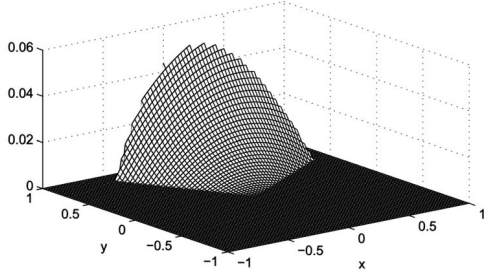


Fig. 3.  $P(C, \alpha, \beta)$  for  $\alpha = \frac{\pi}{6}$  and  $\beta = \frac{2\pi}{3}$ . Note that the displayed distribution is normalized so that the integral of  $P(C, \alpha, \beta)$  sums up to  $P(\alpha, \beta)$  (in this example,  $P(\alpha = \frac{\pi}{6}, \beta = \frac{2\pi}{3}) = 0.0127$ , see (11)).

Equation (2) becomes:

$$P(C, \alpha, \beta) = f_C(r_c, \theta_c) \times \lim_{d\alpha d\beta \rightarrow 0} \frac{1}{d\alpha d\beta} \int_{\alpha-d\alpha/2}^{\alpha+d\alpha/2} \int_{\beta-d\beta/2}^{\beta+d\beta/2} f_B(r_b, \theta_b) r_b dr_b d\theta_b. \quad (6)$$

If the function  $f_B$  is continuous, some computation leads to:

$$P(C, \alpha, \beta) = \begin{cases} 2r_c^2 \frac{\cos(\alpha-\beta) - \cos(\alpha+\beta-2\theta_c)}{3\sin(\alpha-\beta) - \sin(3\alpha-3\beta)} \times \\ f_C(r_c, \theta_c) f_B(r_c \frac{\sin(\theta_c-\beta)}{\sin(\alpha-\beta)}, \alpha) & \text{if } \alpha \leq \theta_c \leq \beta \\ 0 & \text{otherwise.} \end{cases} \quad (7)$$

This probability distribution (7) holds for any continuous distribution of points  $B$  in the plane which represents the prior knowledge of the spatial position of this point.

#### 4 SOLUTION IN THE CASE OF A UNIFORM DISTRIBUTION

We consider here the case of a uniform distribution. We first express  $P(C, \alpha, \beta)$  for this distribution, from which we derive  $P(\alpha, \beta)$ . Finally, we compute  $P(C|\alpha, \beta)$  and  $P(\gamma|\alpha, \beta)$  from which inference will be performed (see Section 6).

This case can be considered as the reference case when no information is available on  $f_B$  and  $f_C$  in (7).

##### 4.1 Uniform Distribution in a Circular Region

Let us now assume that the points  $B$  and  $C$  have a uniform distribution in a circular region of radius  $R$  and origin  $A$ , i.e.:

$$f_C(r, \theta) = f_B(r, \theta) = f(r, \theta) = \begin{cases} \frac{1}{\pi R^2} = K & \text{if } r \leq R \\ 0 & \text{otherwise.} \end{cases} \quad (8)$$

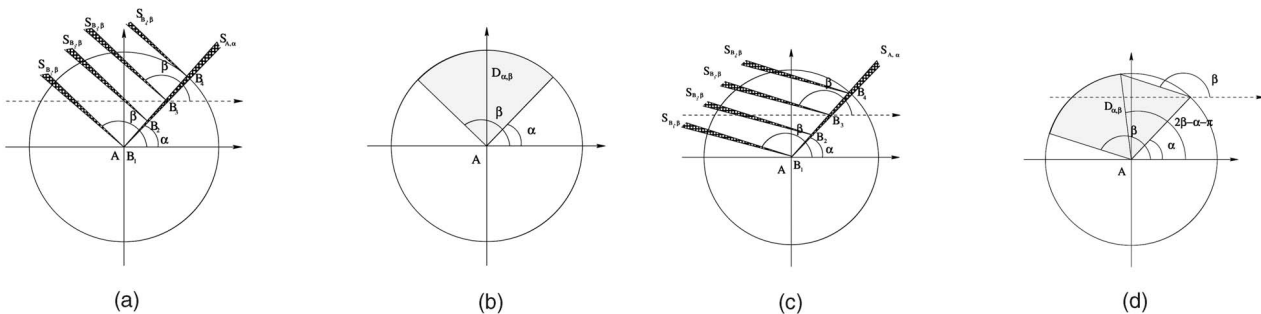


Fig. 5. Definition of the domain  $D_{\alpha, \beta}$  and its two possible shapes.

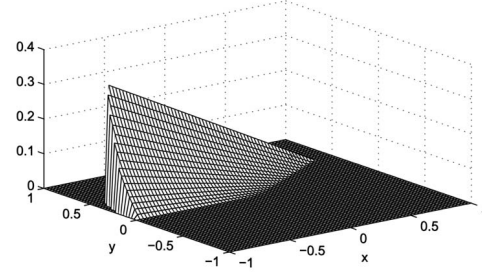


Fig. 4.  $P(C, \alpha, \beta)$  for  $\alpha = \frac{\pi}{6}$  and  $\beta = \pi$  ( $P(\alpha = \frac{\pi}{6}, \beta = \pi) = 0.0586$ , see (12)).

Then, (7) becomes:

$$P(C, \alpha, \beta) = 2r_c^2 K^2 \frac{\cos(\alpha - \beta) - \cos(\alpha + \beta - 2\theta_c)}{3\sin(\alpha - \beta) - \sin(3\alpha - 3\beta)}. \quad (9)$$

Fig. 3 illustrates this distribution for  $\alpha = \frac{\pi}{6}$  and  $\beta = \frac{2\pi}{3}$ , and Fig. 4 for  $\alpha = \frac{\pi}{6}$  and  $\beta = \pi$ .

The probability  $P(C, \alpha, \beta)$  has to be computed in an angular sector of radius  $R$ , thus limiting its support to a region  $D_{\alpha, \beta}$ . This region corresponds to the area covered by the angular sector  $S_{B, \beta}$  of origin  $B$ , angle  $\beta$ , and aperture  $d\beta$  when  $B$  belongs to the angular sector  $S_{A, \alpha}$  (with origin  $A$ , angle  $\alpha$ , and aperture  $d\alpha$ ). This region can have two different shapes depending on  $\beta - \alpha$  (see Fig. 5):

- If  $(\beta - \alpha) \in ]2k\pi, \pi/2 + 2k\pi]$ , then  $D_{\alpha, \beta}$  is a complete angular sector.
- If  $(\beta - \alpha) \in ]\pi/2 + 2k\pi, (2k + 1)\pi[$ , then  $D_{\alpha, \beta}$  consists of a complete angular sector (for  $\theta \in [2\beta - \alpha - \pi, \beta]$ ) and a triangle (for  $\theta \in [\alpha, 2\beta - \alpha - \pi]$ ).
- The case where  $(\beta - \alpha) \in ](2k + 1)\pi, 2(k + 1)\pi]$  is symmetric with respect to the two first ones.

These different cases are illustrated in Fig. 5 and represent the polytope solution of spatial constraints proposed by Spletzer and Taylor [12] in the case of unknown distance.

We can now derive an expression for  $P(\alpha, \beta)$ :

$$P(\alpha, \beta) = \int_{D_{\alpha, \beta}} P(C, \alpha, \beta) dC, \quad (10)$$

which leads to two different expressions depending on the shape of  $D_{\alpha, \beta}$ . In the first case (complete angular sector), we get:

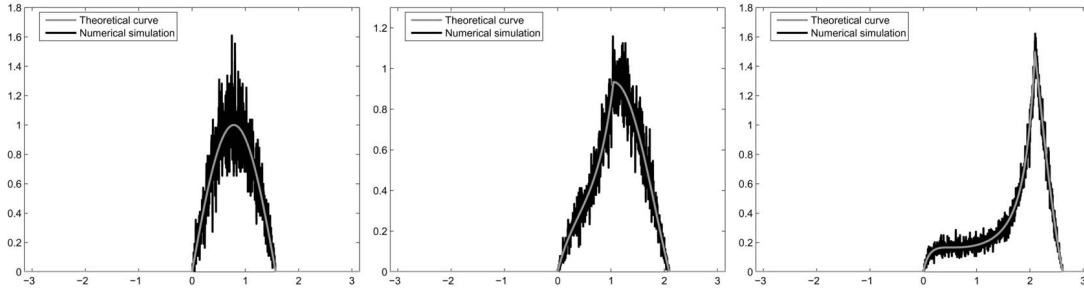


Fig. 6.  $P(\gamma|\alpha, \beta)$  for  $\alpha = 0$  and for  $\beta = \frac{\pi}{2}$ ,  $\frac{2\pi}{3}$ , and  $\frac{5\pi}{6}$ . Gray: theoretical curves. Black: numerical simulations.

$$P(\alpha, \beta) = \frac{(\alpha - \beta) \cos(\alpha - \beta) - \sin(\alpha - \beta)}{2\pi^2 (\sin(3\alpha - 3\beta) - 3 \sin(\alpha - \beta))}, \quad (11)$$

while, in the second case (complete angular sector plus triangle), we get:

$$P(\alpha, \beta) = \frac{5 \sin(\alpha - \beta) + \sin(3\alpha - 3\beta) - 3 \sin(5\alpha - 5\beta) + \sin(7\alpha - 7\beta)}{8\pi^2 (10 \sin(\alpha - \beta) - 5 \sin(3\alpha - 3\beta) + \sin(5\alpha - 5\beta))} + \frac{2(\beta - \alpha - \pi) \cos(\alpha - \beta) - \sin(\alpha - \beta) + \sin(3\alpha - 3\beta)}{4\pi^2 (\sin(3\alpha - 3\beta) - 3 \sin(\alpha - \beta))}. \quad (12)$$

We note that the probability  $P(\alpha, \beta)$  is normalized so that:

$$\int_0^{2\pi} \int_0^{2\pi} P(\alpha, \beta) d\alpha d\beta = 1. \quad (13)$$

The conditional probability  $P(C|\alpha, \beta)$  is expressed as:

$$P(C|\alpha, \beta) = \begin{cases} K_1 r_c^2 \frac{\cos(\alpha - \beta) - \cos(\alpha + \beta - 2\theta_c)}{3 \sin(\alpha - \beta) - \sin(3\alpha - 3\beta)} & \text{if } C \in D_{\alpha, \beta}, \\ 0 & \text{otherwise,} \end{cases} \quad (14)$$

where:

$$K_1 = \frac{2K^2}{P(\alpha, \beta)}, \quad (15)$$

which takes two different expressions depending on the value of  $\beta - \alpha$ .

If we want now to assess the spatial relations between  $C$  and  $A$ , we need to compute the probability of angle  $\gamma$  (between  $A$  and  $C$ ) conditionally to  $\alpha$  and  $\beta$ :

$$P(\gamma|\alpha, \beta) = \int_{D_{\alpha, \beta}} P(\gamma|C, \alpha, \beta) P(C|\alpha, \beta) dC = \int_{S_{A, \gamma} \cap D_{\alpha, \beta}} P(C|\alpha, \beta) dC, \quad (16)$$

where  $S_{A, \gamma}$  is the angular sector of origin  $A$ , angle  $\gamma$ , and aperture  $d\gamma$ . The probability  $P(\gamma|C, \alpha, \beta)$  is equal to 1 if  $C$  is in this sector and to 0 if it is outside, which explains the formula in (16).

Again, we have to distinguish between two cases:

- If  $(\beta - \alpha) \in ]2k\pi, \pi/2 + 2k\pi]$ , we obtain:

$$P(\gamma|\alpha, \beta) = \begin{cases} K_1 \frac{R^4}{4} \frac{\cos(\alpha - \beta) - \cos(\alpha + \beta - 2\gamma)}{3 \sin(\alpha - \beta) - \sin(3\alpha - 3\beta)} & \text{if } \alpha \leq \gamma \leq \beta, \\ 0 & \text{otherwise.} \end{cases} \quad (17)$$

- If  $(\beta - \alpha) \in ]\pi/2 + 2k\pi, (2k + 1)\pi[$ , we obtain:

$$P(\gamma|\alpha, \beta) = \begin{cases} K_1 \frac{\left( \frac{R \sin(\beta - \alpha)}{\sin(\beta - \gamma)} \right)^4}{4} \times \frac{\cos(\alpha - \beta) - \cos(\alpha + \beta - 2\gamma)}{3 \sin(\alpha - \beta) - \sin(3\alpha - 3\beta)} & \text{if } \alpha \leq \gamma \leq 2\beta - \alpha - \pi, \\ K_1 \frac{R^4}{4} \frac{\cos(\alpha - \beta) - \cos(\alpha + \beta - 2\gamma)}{3 \sin(\alpha - \beta) - \sin(3\alpha - 3\beta)} & \text{if } 2\beta - \alpha - \pi < \gamma \leq \beta, \\ 0 & \text{otherwise.} \end{cases} \quad (18)$$

Fig. 6 illustrates the shape of  $P(\gamma|\alpha, \beta)$  for  $\alpha = \frac{\pi}{6}$  and for  $\beta = \frac{\pi}{2}$ ,  $\frac{2\pi}{3}$ , and  $\frac{5\pi}{6}$ , respectively.

To check this theoretical result, we ran a Monte Carlo simulation, where the position of point  $C$  with respect to point  $A$  is computed according to a uniform distribution of the position of points  $B$  and  $C$ . The superposition of the two curves obtained for a large number of trials ( $10^{10}$ ) are presented in Fig. 6. Very similar shapes are obtained.

In the limit cases where  $\beta = \alpha + k\pi$ , different equations are obtained:

- For even values of  $k$ , we have:

$$P(C|\alpha, \beta) = \begin{cases} \frac{4r_c^2}{R^4} & \text{if } C \in S_{A, \alpha}, \\ 0 & \text{otherwise,} \end{cases} \quad (19)$$

$$P(\gamma|\alpha, \beta) = \begin{cases} 1 & \text{if } \gamma = \alpha + k\pi, \\ 0 & \text{otherwise.} \end{cases} \quad (20)$$

- For odd values of  $k$ , we have:

$$P(C|\alpha, \beta) = \begin{cases} \frac{12(R - r_c)^2}{7R^4} & \text{if } C \in S_{A, \alpha}, \\ \frac{12}{7R^2} & \text{if } C \in S_{A, \alpha + \pi}, \\ 0 & \text{otherwise,} \end{cases} \quad (21)$$

$$P(\gamma|\alpha, \beta) = \begin{cases} \frac{1}{k} & \text{if } \gamma = \alpha + (k - 1)\pi, \\ \frac{6}{7} & \text{if } \gamma = \alpha + k\pi, \\ 0 & \text{otherwise.} \end{cases} \quad (22)$$

## 4.2 Uniform Distribution in a Square Region

In most cases in image processing applications, the solution space represents a rectangular or square region of the plane. So, let us now consider the case of a square region of side length equal to  $2R$ , still with a uniform distribution. The

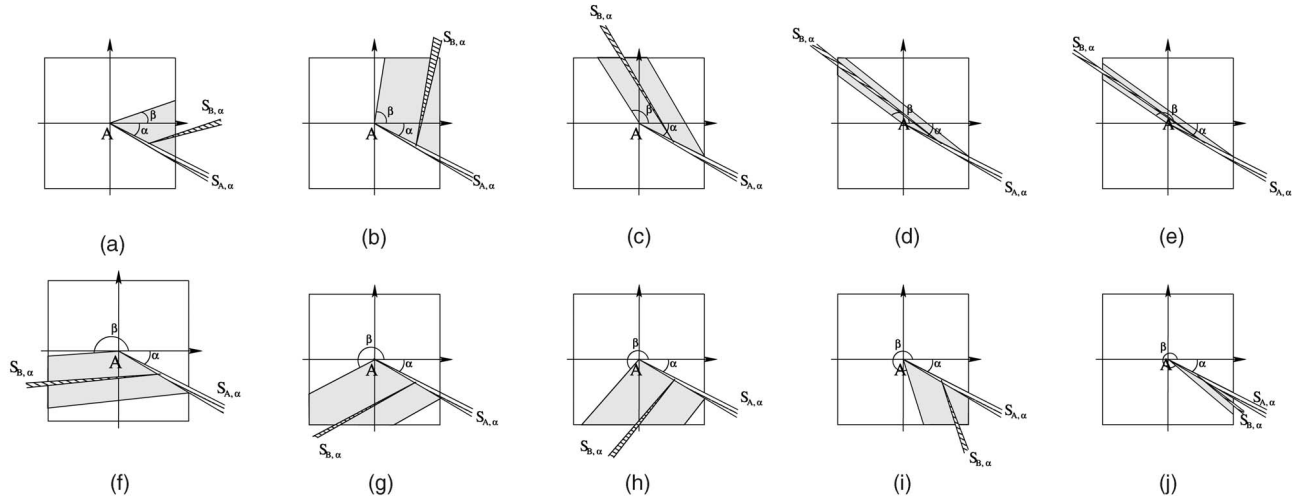


Fig. 7. Possible shapes of  $D_{\alpha, \beta}$  for a square region.

formula for  $P(C, \alpha, \beta)$  remains the same, except for the constant  $K$ , which is now:

$$K = \frac{1}{4R^2}. \quad (23)$$

In this section, we just give the results for  $P(\alpha, \beta)$  and  $P(\gamma|\alpha, \beta)$ . The detailed computation can be found in [32].

The domain  $D_{\alpha, \beta}$  is more complex than for the circular window, and more cases have to be distinguished. We assume that  $\alpha \in [-\pi/4, \pi/4]$  (the other cases are easily deduced) and  $\beta \in [\alpha, \alpha + 2\pi]$  (without loss of generality).

Fig. 7 represents the possible shapes of  $D_{\alpha, \beta}$ . The last five cases are symmetric with respect to the five first ones, therefore, only the five first cases are dealt with in the following:

1. Case  $\alpha < \beta \leq \pi/4$ :

$$P(\gamma|\alpha, \beta) = \frac{1}{32P(\alpha, \beta)} \times \begin{cases} \frac{\cos(\alpha - \beta) - \cos(\alpha + \beta - 2\gamma)}{(3 \sin(\alpha - \beta) - \sin(3\alpha - 3\beta)) \cos^4 \gamma} & \text{if } \alpha \leq \gamma \leq \beta, \\ 0 & \text{otherwise,} \end{cases} \quad (24)$$

with

$$P(\alpha, \beta) = \frac{1}{384 \cos^2 \alpha \cos^2 \beta}. \quad (25)$$

2. Case  $\pi/4 < \beta \leq \pi/2$ :

$$P(\gamma|\alpha, \beta) = \frac{1}{32P(\alpha, \beta)} \times \begin{cases} \frac{\cos(\alpha - \beta) - \cos(\alpha + \beta - 2\gamma)}{(3 \sin(\alpha - \beta) - \sin(3\alpha - 3\beta)) \cos^4 \gamma} & \text{if } \alpha \leq \gamma \leq \pi/4, \\ \frac{\cos(\alpha - \beta) - \cos(\alpha + \beta - 2\gamma)}{(3 \sin(\alpha - \beta) - \sin(3\alpha - 3\beta)) \sin^4 \gamma} & \text{if } \pi/4 < \gamma \leq \beta, \\ 0 & \text{otherwise,} \end{cases} \quad (26)$$

with

$$P(\alpha, \beta) = \cos^2(\alpha + \pi/4) \times \frac{(8 \sin(\alpha - \beta) - 4 \sin(\alpha + \beta) + 4 \cos(\alpha + \beta) + 4 \cos(\alpha - \beta))}{192 \cos^2 \alpha (3 \sin(\alpha - \beta) - \sin(3\alpha - 3\beta))} + \cos(\beta + \pi/4)^2 \times \frac{(8 \sin(\alpha - \beta) + 4 \cos(\alpha - \beta) - 4 \cos(\alpha + \beta) - 4 \sin(\alpha + \beta))}{192 \sin^2 \beta (3 \sin(\alpha - \beta) - \sin(3\alpha - 3\beta))}. \quad (27)$$

3. Case  $\pi/2 < \beta \leq 3\pi/4$ :

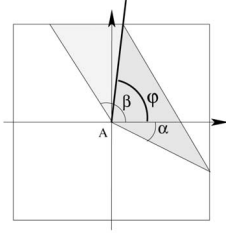
$$P(\gamma|\alpha, \beta) = \frac{1}{32P(\alpha, \beta)} \times \begin{cases} \frac{(\cos(\beta - \alpha) - \cos(\alpha + \beta - 2\gamma)) \sin^4(\alpha - \beta)}{\sin^4(\gamma - \beta) \cos^4 \alpha (3 \sin(\alpha - \beta) - \sin(3\alpha - 3\beta))} & \text{if } \alpha \leq \gamma \leq \varphi, \\ \frac{\cos(\alpha - \beta) - \cos(\alpha + \beta - 2\gamma)}{(3 \sin(\alpha - \beta) - \sin(3\alpha - 3\beta)) \sin^4 \gamma} & \text{if } \varphi < \gamma \leq \beta, \\ 0 & \text{otherwise,} \end{cases} \quad (28)$$

with

$$P(\alpha, \beta) = \frac{\sin^2(\varphi - \alpha) \sin^2(\varphi + \beta)}{128 \cos^4 \alpha (\cos^2 \beta - \cos^2 \varphi)^2} + \sin^2(\beta - \varphi) \times \frac{(3 \cos(\alpha - \beta - \varphi) - \cos(\alpha - \beta + \varphi) - 2 \cos(\alpha + \beta - \varphi))}{192 \sin^3 \varphi \sin^2 \beta (3 \sin(\alpha - \beta) - \sin(3\alpha - 3\beta))}, \quad (29)$$

and  $\varphi$  is the angle limiting the two triangles building the domain  $D_{\alpha, \beta}$  (see Fig. 8):

$$\varphi = \cot^{-1} \left( \frac{\cos \alpha \cos \beta + \sin(\beta - \alpha)}{\cos \alpha \sin \beta} \right). \quad (30)$$

Fig. 8. Support of probability  $P(C, \alpha, \beta)$  in Case  $\pi/2 \leq \beta \leq 3\pi/4$ .

4. Case  $\beta > 3\pi/4$  and  $\varphi \leq 3\pi/4$ :

$$P(\gamma|\alpha, \beta) = \frac{1}{32P(\alpha, \beta)} \times \begin{cases} \frac{(\cos(\beta-\alpha) - \cos(\alpha+\beta-2\gamma)) \sin^4(\beta-\alpha)}{\sin^4(\gamma-\beta) \cos^4 \alpha (3 \sin(\alpha-\beta) - \sin(3\alpha-3\beta))} & \text{if } \alpha \leq \gamma \leq \varphi, \\ \frac{\cos(\alpha-\beta) - \cos(\alpha+\beta-2\gamma)}{(3 \sin(\alpha-\beta) - \sin(3\alpha-3\beta)) \sin^4 \gamma} & \text{if } \varphi < \gamma \leq 3\pi/4, \\ \frac{\cos(\alpha+\beta-2\gamma) - \cos(\beta-\alpha)}{(3 \sin(\beta-\alpha) + \sin(3\alpha-3\beta)) \cos^4 \gamma} & \text{if } 3\pi/4 < \gamma \leq \beta, \\ 0 & \text{otherwise,} \end{cases} \quad (31)$$

with

$$P(\alpha, \beta) = \frac{\sin^2(\varphi - \alpha) \sin^2(\varphi + \beta)}{128 \cos^4 \alpha (\cos^2 \beta - \cos^2 \varphi)^2} + \frac{4 \cos(\alpha - \beta) + 2 \sin(\alpha + \beta) - \sin(\alpha - \beta)}{48(3 \sin(\alpha - \beta) - \sin(3\alpha - 3\beta))} - \frac{\cos \varphi \cos(\alpha - \beta)(2 \cos^2 \varphi - 3) + \cos(\alpha + \beta - 3\varphi)}{96 \sin^3 \varphi (3 \sin(\alpha - \beta) - \sin(3\alpha - 3\beta))} + \frac{\sin(\alpha + \beta) + 2 \sin(\alpha - \beta)}{96 \cos^2 \beta (3 \sin(\alpha - \beta) - \sin(3\alpha - 3\beta))}. \quad (32)$$

5. Case  $\beta < \alpha + \pi$  and  $\varphi > 3\pi/4$ :

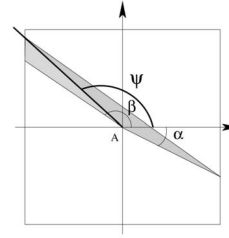
$$P(\gamma|\alpha, \beta) = \frac{1}{32P(\alpha, \beta)} \times \begin{cases} \frac{(\cos(\beta-\alpha) - \cos(\alpha+\beta-2\gamma)) \sin^4(\beta-\alpha)}{\sin^4(\gamma-\beta) \cos^4 \alpha (3 \sin(\alpha-\beta) - \sin(3\alpha-3\beta))} & \text{if } \alpha \leq \gamma \leq \psi, \\ \frac{\cos(\beta-\alpha) - \cos(\alpha+\beta-2\gamma)}{(3 \sin(\alpha-\beta) - \sin(3\alpha-3\beta)) \cos^4 \gamma} & \text{if } \psi < \gamma \leq \beta, \\ 0 & \text{otherwise,} \end{cases} \quad (33)$$

with

$$P(\alpha, \beta) = \frac{\sin^2(\psi - \alpha) \sin^2(\psi + \beta)}{128 \cos^4 \alpha (\cos^2 \beta - \cos^2 \psi)^2} + \sin^2(\beta - \psi) \times \frac{(2 \sin(\beta - \psi + \alpha) - 3 \sin(\beta + \psi - \alpha) - \sin(\beta - \psi - \alpha))}{192 \cos^3 \psi \cos^2 \beta (3 \sin(\alpha - \beta) - \sin(3\alpha - 3\beta))} \quad (34)$$

$$\psi = \cot^{-1} \left( \frac{\cos(\beta - \alpha) + \cos(\beta + \alpha)}{\sin(\beta + \alpha) + 3 \sin(\beta - \alpha)} \right); \quad (35)$$

$\psi$  is the angle limiting the two triangles building the support  $D_{\alpha, \beta}$  of the probability  $P(C, \alpha, \beta)$  (see Fig. 9).

Fig. 9. Support of the probability  $P(C, \alpha, \beta)$  in Cases  $\beta < \alpha + \pi$  and  $\varphi \geq 3\pi/4$ .

## 5 SOLUTION IN THE CASE OF A GAUSSIAN DISTRIBUTION

Since (7) holds for any distribution, the previous computations can be extended to other distributions, such as Gaussian distributions, for instance, which are widely used to model sensor errors and to express uncertain localizations in case of approximate positioning. Let us briefly present the results obtained in this case.

We assume that the point distribution has the following form:

$$f(r, \theta) = \frac{1}{2\pi} e^{-\frac{r^2}{2}}. \quad (36)$$

In the general case where  $\beta \neq \alpha + k\pi$  ( $k \in \mathbb{Z}$ ), we obtain:

$$P(C, \alpha, \beta) = \begin{cases} \frac{r_c^2 (\cos(\alpha - \beta) - \cos(\alpha + \beta - 2\theta_c))}{2\pi^2 (3 \sin(\alpha - \beta) - \sin(3\alpha - 3\beta))} \times e^{-\frac{r_c^2}{2} (1 + \frac{\sin(\theta_c - \beta)}{\sin(\alpha - \beta)})^2} & \text{if } \alpha \leq \theta_c \leq \beta \\ 0 & \text{otherwise.} \end{cases} \quad (37)$$

The derivation of probability  $P(\gamma, \alpha, \beta)$  leads to:

$$P(\gamma, \alpha, \beta) = \begin{cases} \frac{\cos(\alpha - \beta) - \cos(\alpha + \beta - 2\gamma)}{\pi^2 (3 \sin(\alpha - \beta) - \sin(3\alpha - 3\beta)) \frac{\sin^2(\beta - \gamma) + 1}{\sin^2(\beta - \alpha)}} & \text{if } \alpha \leq \gamma \leq \beta \\ 0 & \text{otherwise.} \end{cases} \quad (38)$$

As for the other distributions, the special case of  $\beta = \alpha + k\pi$  ( $k \in \mathbb{Z}$ ) needs specific consideration and different equations are obtained that are not detailed here (see [32] for more results).

Fig. 10 illustrates the obtained results for various values of  $\alpha$  and  $\beta$ .

## 6 BAYESIAN DECISION

We now address the problem of inference, defined here as a decision rule  $\mathcal{D}(\alpha, \beta)$  which assigns to observations  $\alpha$  and  $\beta$  an angle  $\gamma$  corresponding to the directional relative position of point  $C$  with respect to point  $A$ . This decision rule has to minimize a cost function that can be defined in different ways.

For instance, the cost function could be the mean decision error over the complete set of distributions of points. Let us denote by  $\gamma^*$  the exact position of point  $C$  with respect to point  $A$ . The global error probability is expressed as:

$$P_{err} = \int_{-\pi}^{\pi} \int_{-\pi}^{\pi} P(\mathcal{D}(\alpha, \beta) \neq \gamma^*) P(\alpha, \beta) d\alpha d\beta. \quad (39)$$

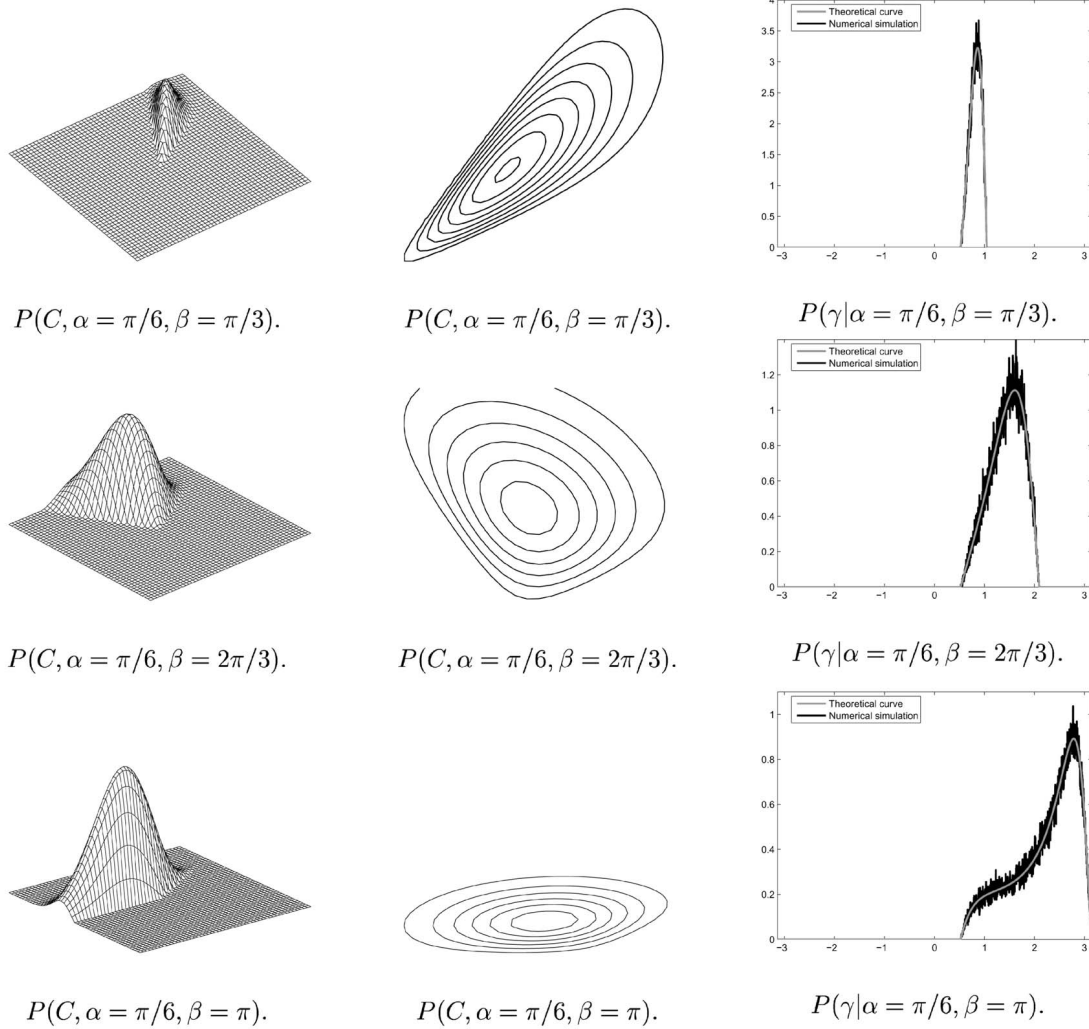


Fig. 10. Examples of  $P(C, \alpha, \beta)$  (surfacing representation on the left and level curves in the middle) and  $P(\gamma|\alpha, \beta)$  (superposition of the theoretical curves and numerical simulation on the right) for various values of  $\alpha$  and  $\beta$  in the case of a Gaussian distribution. The simulated curves were obtained as in Fig. 3.

The probability  $P(\mathcal{D}(\alpha, \beta) = \gamma^*)$  is the probability that  $C$  be in direction  $\mathcal{D}(\alpha, \beta)$  conditionally to  $\alpha$  and  $\beta$ . Therefore, we have:

$$P_{err} = 1 - \int_{-\pi}^{\pi} \int_{-\pi}^{\pi} P(\mathcal{D}(\alpha, \beta)|\alpha, \beta) P(\alpha, \beta) d\alpha d\beta. \quad (40)$$

Minimizing the global error amounts to maximizing  $P(\mathcal{D}(\alpha, \beta)|\alpha, \beta) = P(\gamma|\alpha, \beta)$ .

In the case of a uniform distribution in a circular window of radius  $R$ , the unique maximum of  $P(\gamma|\alpha, \beta)$  is reached for a value of  $\gamma$  (denoted  $\gamma_0$ ) which depends on  $\beta - \alpha$ , which leads to:

$$\mathcal{D}(\alpha, \beta) = \gamma_0 = \begin{cases} \frac{\alpha + \beta}{2} & \text{if } -\frac{2\pi}{3} \leq \beta - \alpha \leq \frac{2\pi}{3}, \\ 2\beta - \alpha - \pi & \text{otherwise.} \end{cases} \quad (41)$$

The first case corresponds to a complete angular sector, for which the probability depends on  $\cos(\alpha + \beta - 2\gamma)$  and has a unique maximum for the given value. The second case corresponds to an incomplete sector, for which the probability depends additionally on  $\frac{\sin(\beta - \alpha)}{\sin(\beta - \gamma)}$ . If  $\beta - \alpha \leq 2\pi/3$ , then the maximum is obtained for the same value as in the first case. Otherwise, it is obtained for  $\gamma = 2\beta - \alpha - \pi$ .

Another possible cost function is the likelihood. Maximizing the likelihood  $P(\alpha, \beta|\gamma)$  amounts to maximize the quantity:

$$\frac{P(\gamma|\alpha, \beta)}{P(\gamma)} \quad (42)$$

and, finally, to maximize the posterior probability  $P(\gamma|\alpha, \beta)$  since no direction is favored. The results are therefore the same as in the previous case.

As a last example, let us consider the minimization of the average decision risk, which generalizes the first criterion by introducing a cost function  $\lambda(\mathcal{D}(\alpha, \beta)|\gamma)$ . Minimizing the average risk amounts to minimizing the conditional risk expressed as:

$$R(\mathcal{D}(\alpha, \beta)|\alpha, \beta) = \int_{-\pi}^{\pi} \lambda(\mathcal{D}(\alpha, \beta)|\gamma) P(\gamma|\alpha, \beta) d\gamma. \quad (43)$$

For instance, if  $\lambda$  is defined as the squared difference  $(\mathcal{D}(\alpha, \beta) - \gamma^*)^2$ , then the minimum is obtained for the following value of  $\gamma$  (for a uniform distribution in a disk):



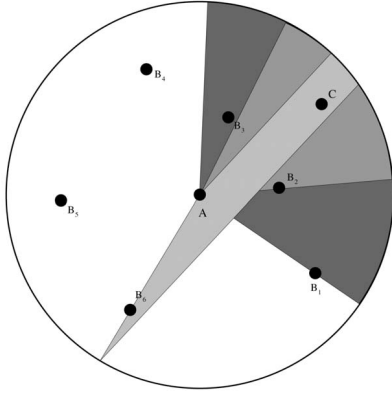


Fig. 11. Example of small objects. The reference point  $A$  is the center of the figure. One instance of point  $C$  and six instances of the intermediary point  $B$  are given ( $B_1 \dots B_6$ ). Angular sectors for  $B_1$ ,  $B_2$ , and  $B_6$  are displayed.

$$\gamma_0 = \begin{cases} \frac{\alpha+\beta}{2} & \text{if } (\beta - \alpha) \in [2k\pi, \pi/2 + 2k\pi], \\ \frac{\psi(\alpha,\beta)}{\varphi(\alpha,\beta)} & \text{if } (\beta - \alpha) \in [2k\pi + \pi/2, (2k+1)\pi], \\ \alpha + \frac{6\pi}{7} & \text{if } \beta = \alpha + \pi, \end{cases} \quad (44)$$

with

$$\begin{aligned} \psi(\alpha, \beta) = & -4((2\beta - \alpha - \pi)^2 - \beta^2 + 1) \cos(\alpha - \beta) \\ & + 5 \cos(3\alpha - 3\beta) - \cos(5\alpha - 5\beta) \\ & - (12\alpha - 20\beta + 8\pi) \sin(\alpha - \beta) \\ & + (8\alpha - 10\beta + 5\pi) \sin(3\alpha - 3\beta) \\ & - (2\beta - \pi) \sin(5\alpha - 5\beta), \end{aligned} \quad (45)$$

and

$$\begin{aligned} \varphi(\alpha, \beta) = & 8(\alpha - \beta + \pi) \cos(\alpha - \beta) \\ & + 8 \sin(\alpha - \beta) - 2 \sin(3\alpha - 3\beta) - 2 \sin(5\alpha - 5\beta). \end{aligned} \quad (46)$$

## 7 ILLUSTRATIVE EXAMPLES

To illustrate how we can use these results, we give two examples of spatial localization. In the first one, we assume that we have no knowledge about the exact position of the points  $B$  and  $C$ , so we have used a uniform distribution for the prior distribution probability  $P(B)$  and  $P(C)$ . In the second example, we use a distribution which reflects the knowledge of the spatial localization of points  $B$  and  $C$ . In this case, the prior distributions are synthetically built from the available knowledge. In real applications, they could be obtained by another approach such as the one used in robot localization [33], [9].

### 7.1 Localization of Mobile Phone Simulation

Let us first consider the problem of inference of directional spatial relations in case of small (quasipoints) objects, for which the previous results can be directly used. An example is given in Fig. 11. The problem addressed in this simulated example is to find the position of point  $C$  with respect to point  $A$ , knowing its position with respect to some reference points  $B_i$  (this is a quite common situation when trying to localize mobile phones). In the absence of any prior knowledge, we assume here a uniform distribution in a circular window.

TABLE 1  
Values of  $\gamma_0$ ,  $|\gamma_0 - \gamma^*|$ , and  $|\beta - \alpha|$  for the Points of Fig. 11

Reference point	$\gamma_0$	$ \gamma_0 - \gamma^* $	$ \beta - \alpha $
$B_1$	0.52	0.12	2.12
$B_2$	0.59	0.05	1.01
$B_3$	0.68	0.04	1.07
$B_4$	0.79	0.15	2.16
$B_5$	0.67	0.03	2.83
$B_6$	0.62	0.02	2.94

For low (close to 0) or large (close to  $\pi$ ) values of  $|\beta - \alpha|$ , the error  $|\gamma_0 - \gamma^*|$  is small.

In this simulated example, the solution is known:  $\gamma^* = 0.64 \text{ rad}$ . The values for  $\gamma_0$  (obtained with inference based on minimization of error probability, see (41)),  $|\gamma_0 - \gamma^*|$  (estimation error with respect to the true value) and  $|\beta - \alpha|$  are given in Table 1 for the six instances  $B_i$  of  $B$ .

The smallest estimation errors occur for both low and large values of  $|\beta - \alpha|$ . This was expected since the localization is more difficult if the angular sector  $D_{\alpha,\beta}$  is larger, which results from average values of  $|\beta - \alpha|$ .

The error probability decreases if several intermediary objects are used, by combining the corresponding probabilities  $P(\gamma|\alpha, \beta)$ . The probabilistic distributions are given in Fig. 12, each curve corresponding to one of the  $B_i$ . All curves have a peak close to the exact value of  $\gamma^*$  (i.e., 0.64). They are more or less spread depending on the uncertainty that remains in the location (i.e., depending on  $|\beta - \alpha|$ ). For instance, the angular sector for  $B_6$  is reduced (see Fig. 11), which leads to a good estimation (Fig. 12). The product of these probabilities clearly tends towards a Dirac function (corresponding to an intersection of several domains  $D_{\alpha,\beta}$ ), showing that using several reference points improves the localization, as expected. Note that if many point measurements are available, which may be prone to errors, methods dealing with outliers should be added in the procedure [34].

The idea briefly presented here was further explored for mobile location in wireless communication in [35].

### 7.2 Georeferencing in a City

In this example, we address a more complex situation, where we have to localize a point, here, the ENST (Ecole Nationale Supérieure des Télécommunications), in a real city map, based on knowledge about relations to other geographical locations (subway stations in our example). This example aims at showing how qualitative information may be used in improving a localization problem.

We assume that two fixed points are known: "Place d'Italie" and "Porte d'Italie" (see the map<sup>2</sup> of the considered area in Fig. 13). They will be referred to as points  $A_1$  and  $A_2$  and will successively play the role of the starting point  $A$  according to the notations of Section 3. The different pieces of knowledge which will be used in the sequel are as follows:

2. <http://www.maporama.com>.

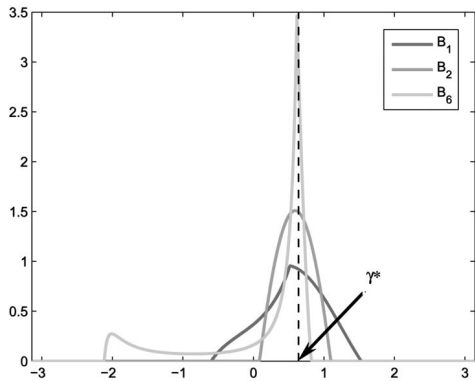


Fig. 12. Probability distributions  $P(\gamma|\alpha, \beta)$  obtained for some points of Fig. 11. The vertical dashed line indicates the correct solution.

- **K1:** "Tolbiac" is in the direction of  $A_2$  with respect to  $A_1$ .
- **K'1:** "Tolbiac" is in the direction of  $A_1$  with respect to  $A_2$ .
- **K2:** ENST is West of "Tolbiac."
- **K3:** ENST is not far from "Place d'Italie."
- **K4:** "Tolbiac" is not far from the mid point of the segment  $A_1A_2$  ("Place d'Italie" - "Porte d'Italie").

Such pieces of knowledge, expressed as linguistic expressions, can be easily understood by human beings, despite their imprecision, thanks to links between language and cognition [1]. Using them in our framework requires us to quantify them in some way. Each piece of knowledge is therefore expressed as a probability distribution. Although this may sound rather ad hoc, the distributions have a sufficiently large support to correspond to what is intuitively understood.

In order to exploit the results of Section 3, in a first experiment, we make use only of **K1** and **K2**. We start from  $A_1$  ("Place d'Italie") as point A. "Tolbiac" is the unknown intermediary point B, and "ENST" the point C we are trying to localize. At this point, no knowledge is available on the position of ENST, thus, we assume a uniform distribution inside the map. By applying the equations derived in Section 4.2, we obtain the distribution described in Fig. 14a. The solution given by the maximum posterior probability provides, as a candidate for ENST, the point in the bottom-left corner. Note that a point at the border of the admission domain is likely to be obtained with the uniform distribution assumption as demonstrated in Sections 3 and 4.2 (see, in particular, (7) and Fig. 7b). With such a weak information, the obtained result is rather poor and disappointing.

To improve the positioning, we now make use of knowledge **K3**, along with **K1** and **K2**. In order to translate quantitatively the linguistic expression "not far from," we adopt a Gaussian probability distribution for  $P(C)$ , centered at  $A_1$  with a standard deviation equal to 1km (Fig. 14b), instead of the uniform distribution. This corresponds to the usual way of communicating approximate distance information expressed as linguistic expressions: For instance, when indicating a distance, even using a crisp number, the meaning is not exactly this number, but it should be understood in a smoother way, expressed here by the choice of the Gaussian. A better solution is now obtained (Fig. 14c), which is no longer peaking at the border of the admissible domain. The maximum of the distribution is somewhat closer to what is expected.

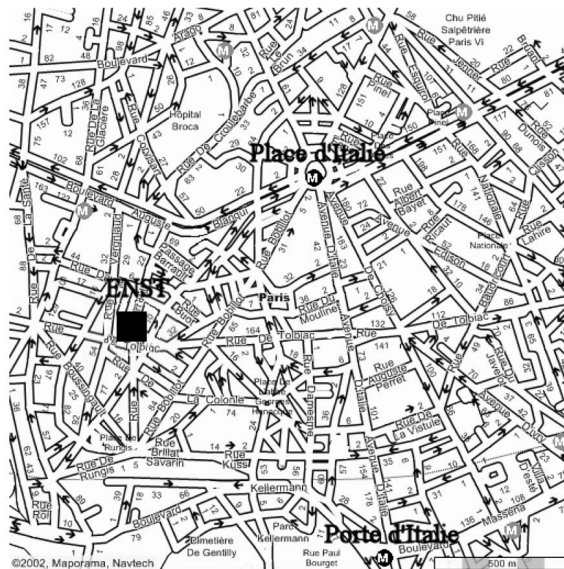


Fig. 13. Map of an area around ENST (square) in Paris. Two reference points, "Place d'Italie" and "Porte d'Italie," are indicated too.

A second improvement may be obtained by providing a more realistic information on the intermediary point "Tolbiac." For this purpose, we make use of knowledge **K4**. The prior probability distribution of this intermediary point B is now no longer uniform in the direction of  $A_2$  with respect to  $A_1$ . As for **K3**, we choose for the distribution of B according to **K4** a Gaussian distribution centered at the midpoint of  $A_1A_2$  (Fig. 14d). The use of the starting point  $A_1$  and the 4 pieces of knowledge **K1**, **K2**, **K3**, and **K4**, provides a solution which is closer to the true solution (Fig. 14e).

From this series of examples, the exact position of "Porte d'Italie" has never been used. Can this information improve our estimate? Let us take  $A_2$  as starting point A and evaluate the position of ENST from **K'1**, **K2**, and **K4** and by using the last distribution obtained in Fig. 14e as prior distribution for ENST. We obtain a new distribution, better than the previous ones, presented in Fig. 14f. The solution becomes more accurate and the maximum of the probability is very close to the exact position of ENST.

These series of examples illustrate the contribution of every piece of information to the modeling of the posterior probability. The compounding of probabilities, made under the Bayesian formalism, provides a convenient framework. One may discuss the translation of every qualitative piece of knowledge into a quantitative prior probability distribution and substitute any distribution to the Gaussian or uniform distributions when some evidence advocates it. It appears from these results that the quality of the results is only depending on the quality of the prior information and not on the way the knowledge is processed. Improving constraints and knowledge allows to refine the positioning.

## 8 CONCLUSION

In the field of spatial reasoning and inference of spatial relations, we proposed in this paper a probabilistic formulation for this problem in the case of punctual objects. We derived analytical formulae in case of circular and square domains and for different types of point distributions. The joint probability  $P(C, \alpha, \beta)$  is valid for any

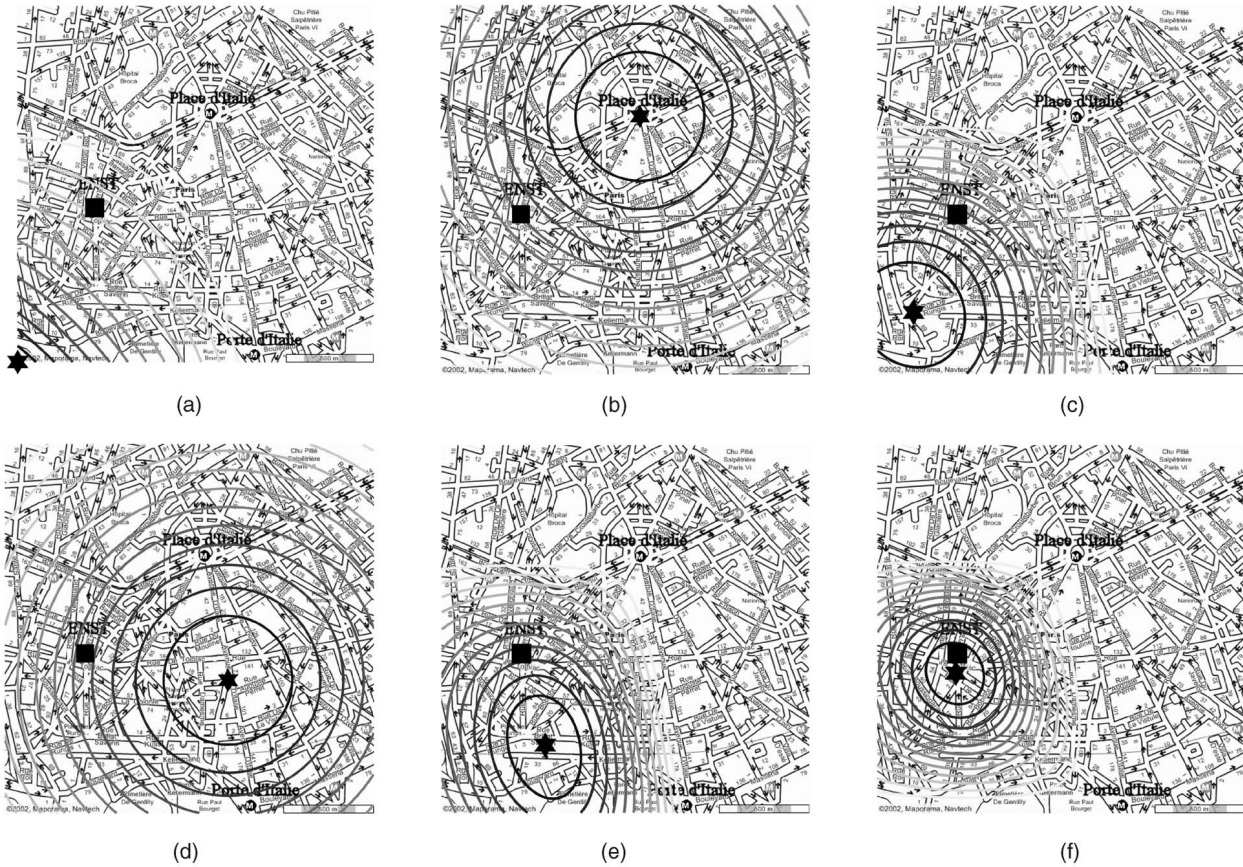


Fig. 14. Combination of available knowledge: (a) distribution of point  $C$  (ENST) according to  $K_1$  and  $K_2$  (the probability distribution is displayed as level curves with increasing intensity and the maximum value is represented by a star); (b) modeling  $K_3$ ; (c) distribution of  $C$  given  $K_1$ ,  $K_2$ , and  $K_3$ ; (d) modeling  $K_4$ ; (e) distribution of  $C$  given  $K_1$ ,  $K_2$ ,  $K_3$ , and  $K_4$ ; and (f) distribution of  $C$  given  $K_1$ ,  $K_2$ , and  $K_4$  using the result of (e) as prior knowledge on  $C$ .

distribution, while the conditional probability  $P(\gamma|\alpha, \beta)$  has to be derived specifically for each distribution.

In the general case, where we have to deal with spatial entities having any shape and spatial extension, two cases have to be distinguished. The first one corresponds to quite compact objects, either of small size or far from each other. As a first approximation, such objects can be considered as points and the proposed approach applies directly. The second case corresponds to extended objects, for which the size is too large with respect to the distance between them to allow us to consider them as points. In such cases, the computation on points is no more sufficient. One possibility consists in combining the probability distribution with angle histograms [21]. This approach has been investigated in [32], but still needs to be further developed. In particular, estimating the conditional probability  $P(\beta|\alpha)$  seems to be a necessary step.

Extensions to 3D are also possible, but the derivations are likely to be much more complex since positioning a point in a 3D space requires two angles instead of one. This is left for future work.

In cases where the knowledge is deduced from many measurements, not only the uncertainty due to errors should be taken into account, but also possible bias or outliers. Robust methods should then be combined with our approach [34].

In the examples we have presented, we focused upon relating the position of one point  $A$  to another point  $C$  through an intermediary location  $B$ . We also demonstrated this for multiple intermediaries taken one at a time. An

interesting extension would be to deal with cases where we have a list of constraints relating the relative positions across a large group of points (or objects) in order to derive a probability distribution for each point simultaneously conditioned on all of the relative spatial information. Such a problem was addressed in [12], where an efficient method is proposed to determine the domain of all the possible solutions. An extension of our work could provide an information on the probability of every point in this admissible region.

Foreseen applications concern, for instance, the localization of mobile phones as shown in our first simulated example, and experienced in [35]. This application could be useful typically in rescue issues.

## REFERENCES

- [1] B. Landau and R. Jackendoff, "What' and 'Where' in Spatial Language and Spatial Cognition," *Behavioral and Brain Sciences*, vol. 16, pp. 217-265, 1993.
- [2] H.F. Durrant-Whyte, "Uncertain Geometry in Robotics," *IEEE J. Robotics and Automation*, vol. 4, no. 1, pp. 23-31, Feb. 1988.
- [3] J. Borenstein, H.R. Everett, and L. Feng, *Where am I? Sensor and Methods for Mobile Robot Positioning*. Univ. of Michigan, 1996.
- [4] R. Smith, M. Self, and P. Cheeseman, *Estimating Uncertain Spatial Relationships in Robotics*, chapter 3, pp. 167-193, Springer-Verlag, 1990.
- [5] R. Chatila and J.-P. Laumond, "Position Referencing and Consistent World Modeling for Mobile Robots," *Proc. IEEE Int'l Conf. Robotics and Automation*, pp. 138-145, 1985.

- [6] R. Smith and P. Cheeseman, "On the Representation and Estimation of Spatial Uncertainty," *The Int'l J. Robotics Research*, vol. 5, no. 4, pp. 56-68, 1987.
- [7] H.P. Moravec and A. Elfes, "High Resolution Maps from Wide Angle Sonar," *Proc. IEEE Int'l Conf. Robotics and Automation*, pp. 116-121, 1985.
- [8] W. Burgard, D. Fox, D. Hennig, and T. Schmidt, "Estimating the Absolute Position of a Mobile Robot Using Position Probability Grids," *Proc. 14th Nat'l Conf. Artificial Intelligence (AAAI)*, vol. 2, pp. 896-901, 1996.
- [9] D. Fox, W. Burgard, and S. Thrun, "Active Markov Localization for Mobile Robots," *Robotics and Autonomous Systems*, vol. 25, pp. 195-207, 1998.
- [10] J.J. Leonard and H.F. Durrant-Whyte, "Mobile Robot Localization by Tracking Geometric Beacons," *IEEE Trans. Robotics and Automation*, vol. 7, no. 3, pp. 376-382, June 1991.
- [11] M. Betke and L. Gurvits, "Mobile Robot Localization Using Landmarks," *IEEE Trans. Robotics and Automation*, vol. 13, no. 2, pp. 251-263, 1997.
- [12] J.R. Spletzer and C.J. Taylor, "A Bounded Uncertainty Approach to Multi-Robot Localization," *Proc. Int'l Conf. Intelligent Robots and Systems*, pp. 1258-1265, 2003.
- [13] L. Doherty, K.S.J. Pister, and L. El Ghaoui, "Convex Position Estimation in Wireless Sensor Networks," *Proc. IEEE Infocom*, vol. 3, pp. 1655-1663, 2001.
- [14] L. Vieu, "Spatial Representation and Reasoning in Artificial Intelligence," *Spatial and Temporal Reasoning*, pp. 5-41. Dordrecht, Kluwer, 1997.
- [15] A.G. Cohn, "Qualitative Spatial Representations," *Proc. IJCAI99 Workshop Adaptive Spatial Representations of Dynamic Environments*, pp. 33-52, 1999.
- [16] G. Ligozat, "Reasoning about Cardinal Directions," *J. Visual Languages and Computing*, vol. 9, pp. 23-44, 1998.
- [17] J.F. Allen, "Maintaining Knowledge about Temporal Intervals," *Comm. ACM*, vol. 26, no. 11, pp. 832-843, 1983.
- [18] S.K. Chang, Q.Y. Shi, and C.W. Yan, "Iconic Indexing by 2D Strings," *IEEE Trans. Pattern Analysis and Machine Intelligence*, vol. 9, no. 3, pp. 413-428, May 1987.
- [19] C. Freksa and K. Zimmermann, "On the Utilization of Spatial Structures for Cognitively Plausible and Efficient Reasoning," *Proc. IEEE Int'l Conf. Systems, Man, and Cybernetics*, pp. 261-266, Oct. 1992.
- [20] J. Freeman, "The Modeling of Spatial Relations," *Computer Graphics and Image Processing*, vol. 4, pp. 156-171, 1975.
- [21] K. Miyajima and A. Ralescu, "Spatial Organization in 2D Segmented Images: Representation and Recognition of Primitive Spatial Relations," *Fuzzy Sets and Systems*, vol. 65, pp. 225-236, 1994.
- [22] J.M. Keller and X. Wang, "Comparison of Spatial Relation Definitions in Computer Vision," *Proc. Third Int'l Symp. Uncertainty Modeling and Analysis and Ann. Conf. North Am. Fuzzy Information Processing Soc.*, pp. 679-684, Sept. 1995.
- [23] P. Matsakis and L. Wendling, "A New Way to Represent the Relative Position between Areal Objects," *IEEE Trans. Pattern Analysis and Machine Intelligence*, vol. 21, no. 7, pp. 634-642, July 1999.
- [24] J.M. Keller and X. Wang, "Learning Spatial Relationships in Computer Vision," *Proc. Int'l Conf. Fuzzy Systems*, pp. 118-124, 1996.
- [25] L.T. Koczy, "On the Description of Relative Position of Fuzzy Patterns," *Pattern Recognition Letters*, vol. 8, pp. 21-28, 1988.
- [26] I. Bloch, "Fuzzy Relative Position between Objects in Image Processing: A Morphological Approach," *IEEE Trans. Pattern Analysis and Machine Intelligence*, vol. 21, no. 7, pp. 657-664, July 1999.
- [27] I. Bloch and A. Ralescu, "Directional Relative Position between Objects in Image Processing: A Comparison between Fuzzy Approaches," *Pattern Recognition*, vol. 36, pp. 1563-1582, 2003.
- [28] S. Dutta, "Approximate Spatial Reasoning: Integrating Qualitative and Quantitative Constraints," *Int'l J. Approximate Reasoning*, vol. 5, pp. 307-331, 1991.
- [29] *Fuzzy Logic Techniques for Autonomous Vehicle Navigation*, Studies in Fuzziness and Soft Computing, D. Driankov and A. Saffiotti, eds. Springer-Physica Verlag, 2001.
- [30] L. Talmy, "How Language Structures Space," *Spatial Orientation: Theory, Research and Application*, H.L. Pick and L.P. Acredolo, eds. New York: Plenum Press, 1983.
- [31] E.T. Jaynes, "Information Theory and Statistical Mechanics," *Physical Rev.*, vol. 106, no. 4, pp. 620-630, 1957.

- [32] R. Dehak, "Inférence Quantitative des Relations Spatiales Directionnelles," PhD thesis, Ecole Nationale Supérieure des Télécommunications, Paris, France, 2002E043, 2002.
- [33] R. Simmons and S. Koenig, "Probabilistic Robot Navigation in Partially Observable Environments," *Proc. Int'l Joint Conf. Artificial Intelligence*, pp. 1080-1087, 1995.
- [34] P.J. Rousseeuw and A.M. Leroy, *Robust Regression and Outlier Detection*. New York: John Wiley, 1987.
- [35] E. Grosicki, K. Abed-Meraim, and R. Dehak, "A Novel Method to Fight the Non-Line-of-Sight Error in AOA Measurements for Mobile Location," *Proc. IEEE Int'l Conf. Comm.*, vol. 5, pp. 2794-2798, 2004.



**Sidi Mohammed Réda Dehak** received the PhD degree in signal and image processing from Ecole Nationale Supérieure des Télécommunications in 2002, the MS degree in signal and image processing in 1998 from the Institut National des Sciences Appliquées (INSA), Lyon, France, and the Engineer degree in computer science in 1997 from Université des Sciences et de la Technologie d'Oran, Algeria. He is an assistant professor in computer science and a member of the EPITA Research and Development Laboratory (LRDE). His research interests include fuzzy sets theory, decision theory, pattern recognition, spatial relations, and spatial reasoning. He is a member of the IEEE.



**Isabelle Bloch** is a professor at ENST (Signal and Image Processing Department). Her research interests include 3D image and object processing, 3D and fuzzy mathematical morphology, decision theory, information fusion, fuzzy set theory, belief function theory, structural pattern recognition, spatial reasoning, and medical imaging. She is a member of the IEEE.



**Henri Maître** received the engineering degree from the Ecole Centrale de Lyon, France (1971), and the Docteur es Sciences degree in physics from the University of Paris VI (1982). He has taught digital picture processing since 1973 at the Ecole Nationale Supérieure des Télécommunications (Telecom Paris) in Paris where he is a professor. His research includes work on image analysis, image understanding and computer vision, and applications in the domains of satellite and aerial image processing. He is a member of the IEEE.

► For more information on this or any other computing topic, please visit our Digital Library at [www.computer.org/publications/dlib](http://www.computer.org/publications/dlib).